Electron paramagnetic resonance in sodium ammonium sulphate dihydrate of radicals produced by X-irradiation

1993 J. Phys.: Condens. Matter 5 459

(http://iopscience.iop.org/0953-8984/5/4/013)

J. Phys.: Condens. Matter 5 (1993) 459–468. Printed in the UK

Electron paramagnetic resonance in sodium ammonium sulphate dihydrate of radicals produced by x-irradiation

J M Baker†, M I Cook†, A L Tronconi†, J Kuriata‡ and L Sadlowski‡
† Oxford Physics, Clarendon Laboratory, Parks Road, Oxford OX1 3PU, UK
‡ Instytut Fizyki, Politechnika Szczecinska, Szczecin, Poland

Received 26 October 1992

Abstract. X-irradiation of sodium ammonium sulphate dihydrate produces a complex electron paramagnetic resonance spectrum indicating the production of five, or possibly six, different radicals. The relative concentration of these appears to depend upon the crystal growth, but not on subsequent treatment. Those with extensive hyperfine structure have been identified as NH_3^+ and NH^+. Identification of the others, presumably derived from the SO_4 group, is more tentative. The only change in the spectrum observed on cooling through the ferroelectric phase transition is a small doubling of the outermost hyperfine lines of NH_4^+, which suggests that all of the radicals produced are somewhat detached from the lattice, and so not very susceptible to changes in its structure.

1. Introduction

In order to understand the mechanisms of a phase transition in a solid, it is important to know the structural changes which occur at the transition. One technique which may be used to discover this information is electron paramagnetic resonance (EPR) of either (i) probe transition metal ions doped into the crystals, or (ii) paramagnetic radicals produced by irradiation, because the spectra of such species are sensitive to the nature and symmetry of their surroundings (Owens 1985).

In this paper we discuss the application of this technique to $NaNH_4SO_4{\cdot}2H_2O$ (which we refer to hereafter by the acronym SASD, sodium ammonium sulphate dihydrate), known in mineral form as lecontite, which becomes ferroelectric at 101 K, and has a further phase transition at 92 K (Makita and Sekido 1965).

This paper is concerned with the EPR spectrum of radicals produced by x-irradiation. A preliminary account of this work, and of the spectra of Cr^{3+} impurities in SASD has been given by Baker *et al* (1992). Some previous EPR measurements in SASD have been reported by Sadlowski *et al* (1985) in single crystals irradiated for a few hours with x-rays from a Co cathode using 40 kV and 20 mA, or with 13 MeV electrons using a linear accelerator. A rather poorly resolved spectrum, whose angular variation was difficult to measure, was attributed to NH_3^+ and $(SO_4)^-$ radicals. The intensity of the EPR spectrum was linearly proportional to the radiation dose up to 3 Mrad. The radicals were stable for several months at room temperature, but were destroyed by heating the crystal to 333 K. EPR has been also measured between 300 and 77 K by Lakshmana Rao *et al* (1990) in SASD doped with Cu^{2+}.

SASD and the isomorphic material sodium ammonium selenate dihydrate (SASeD) are orthorhombic with space group $P2_12_12_1$ and four molecules in the unit cell

0953-8984/93/040459+10$07.50

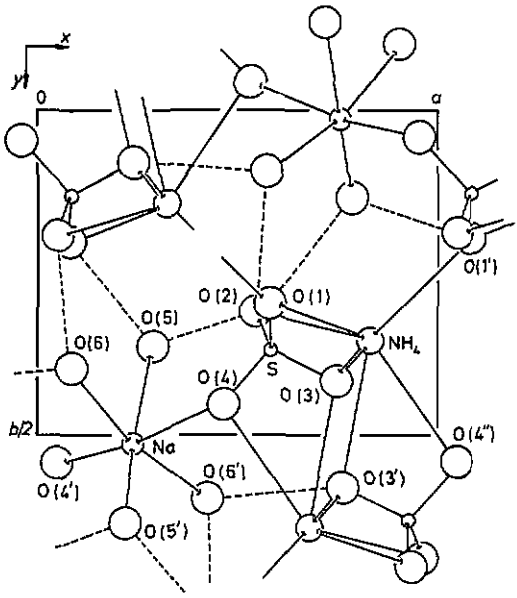

Figure 1. The crystal structure of SASD viewed along [001].

in the paraelectric phase (Corazzo *et al* 1967), and $P2_1$ in the ferroelectric phase (Aleksandrov *et al* 1978). Figure 1 shows the structure of SASD, which may be regarded as chains of NaO_6 octahedra, sharing three O atoms on a face, approximately aligned along [001], interlaced with chains of (NH_4^+)–(SO_4^{2-})–(NH_4^+), the two types of chain being linked by sharing one O in the SO_4 tetrahedra and hydrogen bonds. Chains containing Na are quite separate, they do not share the same SO_4 tetrahedra. The materials are of interest because they contain NH_4 and H_2O, both of which have been found to be active in the ferroelectric transition in similar materials (Genin and O'Reilly 1969).

However, Genin and O'Reilly have shown using proton and deuteron NMR in SASD that the H–H and D–D directions for the water molecules do not change at either of the transition temperatures, suggesting that the water molecules are not involved with the ferroelectricity. Further, lack of change in the deuteron NMR of ND_4^+ shows that the radical does not undergo distortion at either of the transitions; and the quadrupole interaction shows that ND_4 is a perfect tetrahedron. However, at 111 K, there is a change in the activation energy for rotation about the threefold axis of NH_4, as detected by proton relaxation rates; and also a marked separation into two types of Na site as shown by a splitting of the quadrupole satellites of the ^{23}Na NMR for external field parallel to [100], though there are no similar effects at 92 K. The four Na sites, equivalent under $P2_12_12_1$ split into two pairs equivalent under $P2_1$ for $T < T_c$. The absence of involvement of motion of NH_4 in the ferroelectricity is confirmed by the lack of a large change in T_c on deuteration of the material.

It is suggested by Ramani and Srinivasan (1981) that at room temperature the rapid re-orientation of NH_4 and SO_4 radicals results in a structure dominated by ionic bonding. Both motions slow down as T is reduced, so allowing hydrogen bonding to play a more prominent role, with consequent atomic displacements. NH_4 is supposed to slow first as T is reduced, leaving the slowing of SO_4 to determine T_c: ionic displacements in the sodium–oxygen octahedra and consequent displacements in the

tetrahedral groups are supposed to lead to the ferroelectricity.

EPR has been studied by Ramani and Srinivasan (1981) in SASeD, where the ferroelectric transition temperature is 180 K. Irradiation with ^{60}Co γ-rays produced the radicals SeO_4^-, SeO_3^- and SeO_2^-, identified from their g-matrices and the ^{77}Se hyperfine matrices. The involvement of SeO_4 in the ferroelectric transition is shown by the change of g-matrix for SeO_4^- from isotropic at room temperature to rhombic close to T_c. This contrasts with the g-matrices of SeO_3^- and SeO_4^-, which show no change at T_c.

2. Experimental details

EPR was measured in standard spectrometers at four microwave frequencies near 9.4, 17, 24 and 35 GHz all using 115 kHz modulation of the applied magnetic field and subsequent phase sensitive detection. The applied magnetic field $\boldsymbol{B}$ could be rotated about a vertical axis to investigate the angular dependence of EPR in a horizontal plane in the sample. The microwave cavity containing the sample could be operated either at room temperature, in a bath of refrigerant at 77 K or 4 K, or in a Oxford Instruments CF200 helium flow cryostat for continuous variation of temperature from 4 to 300 K.

Large, good quality, single crystals of SASD were grown from a saturated aqueous solution of equimolar ratio $(NH_4)_2SO_4$ and Na_2SO_4 by slow evaporation, as the temperature was decreased at 0.4 K per day from 304 to 299 K. Also, some smaller crystals of adequate quality and good morphology were grown by allowing a saturated solution to evaporate at room temperature without careful temperature control. Some crystals were grown using $(NH_4)_2SO_4$ which was isotopically enriched to 99.5% ^{15}N. Others (batch 1) were grown using 99.9% $(ND_4)_2SO_4$, dissolved with anhydrous $NaSO_4$ in 99.9%D_2O, but these became quite heavily contaminated with protons. As this was thought to be due to exposure to atmospheric moisture, a second batch (2) was grown using carefully dried $NaSO_4$ and taking care that atmospheric moisture was excluded from the dessicator. Although less contaminated, this batch also contained a significant proton fraction.

Crystals of SASD from aqueous solution have well formed faces. In spite of the lattice parameters having ratios close to those of simple numbers, there was no evidence of twinning of the crystals. The symmetry axes are easily recognized from the morphology of the crystals. Well formed (100), (010) and (001) faces made it easy to cut cubic specimens of side approximately 2 mm with faces oriented to better than 1°, and facilitated the mounting of the crystals, allowing measurement in these symmetry planes. Any slight misorientation of the plane could be compensated by tilting the cryostat through a small angle. As the EPR spectra measured showed no site symmetry, each site gives rise to four spectra related by the symmetry operations of the crystal. Most measurements were therefore made in the planes of reflection symmetry where sites are equivalent in pairs; and the simplest spectra occur when the external field is along one of the crystal axes, when all four sites are equivalent.

3. The observed EPR spectrum

Even for B along a crystal axis, the EPR spectrum produced by x-irradiation for eight hours using a tungsten anode at 45 kV and 40 mA was quite complicated at room

temperature. Before attempting to understand the changes which occur on cooling the crystal through the transitions, the spectrum was studied at room temperature. This comprised some strong lines near $g = 2$, and an extensive hyperfine structure with overall range of about 150 mT. All of the radicals formed by x-irradiation correspond to $S = \frac{1}{2}$ and are described by a spin Hamiltonian

$$H = \mu_B \boldsymbol{S} \cdot \mathbf{g} \cdot \boldsymbol{B} + \boldsymbol{S} \cdot \sum_j \mathbf{A}_j \cdot \boldsymbol{I}_j$$

where the summation is over any nuclei which have a hyperfine interaction with the unpaired electron. The nuclei in the crystal which might give rise to such hyperfine structure are $^1H(I = \frac{1}{2})$, $^{14}N(I = 1)$ and $^{27}Na(I = \frac{3}{2})$: the natural abundance of the odd isotopes of O and S is too small to be significant. We have also used some crystals with isotopic substitution of $^2D(I = 1)$ and $^{15}N(I = \frac{1}{2})$.

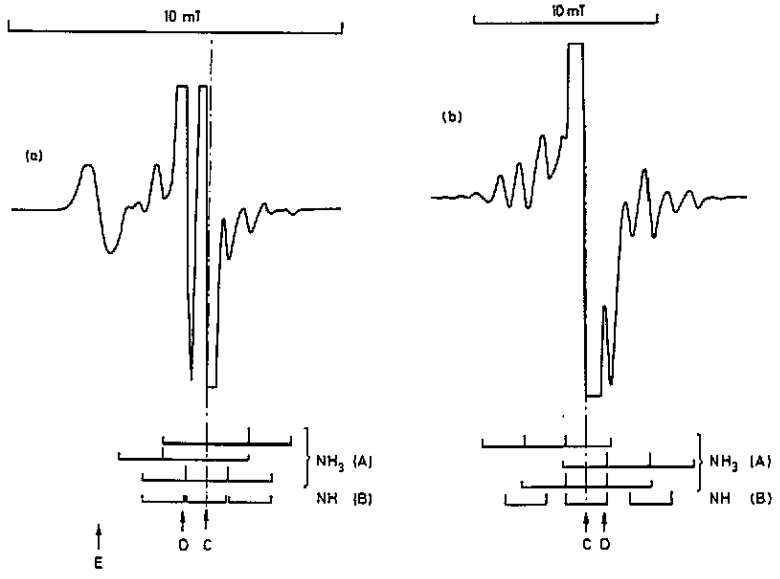

Figure 2. EPR spectra at 300 K of x-irradiated SASD at about 17 GHz for $\boldsymbol{B}$ along the (*a*) [100] and (*b*) [001].

Close to the crystal axis the spectrum shown in figures 2 and 3 had reasonably resolved structure which became increasingly unclear as $\boldsymbol{B}$ was rotated away from these directions. Even though measurements were made every few degrees, it was impossible to follow unambiguously the angular variation of lines which crossed one another and changed intensity. The only lines which could be followed easily throughout their angular variation were the stronger lines at the centre of the spectrum with no hyperfine structure, and the outermost hyperfine lines which did not cross other lines in the spectrum. Even the latter become weak in some directions. Following the angular variation in the symmetry planes would be complicated by small misorientations of the plane which would cause doubling of the lines to an extent dependent upon their anisotropy. Hence, the most reliable information comes for $\boldsymbol{B}$

along the orthorhombic crystal axes, where at least twofold degeneracy is ensured by rotation of B: the similarity of spectra in different mountings of the same sample or for different samples, suggest that misorientation does not produce severe spectral distortion. Furthermore, comparison of the spectra for [100], [010] and [001] indicates that there is no twinning of the crystals.

Several attempts were made to simplify the spectrum:

(i) The temperature of measurement was varied to see whether differential saturation would change relative intensities.

(ii) The irradiation conditions were varied to look for changes in the relative rates of production of different radicals.

(iii) The temperature of the samples was raised slowly above room temperature, and the spectrum examined from time to time, to attempt to anneal spectra differentially.

None of these was successful in making any difference to the spectra.

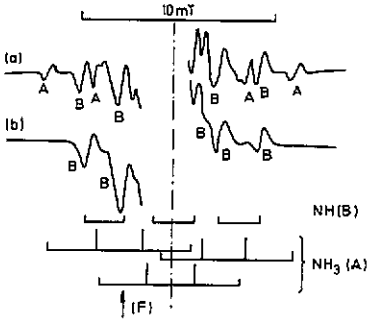

Figure 3. EPR spectrum at 300 K of x-irradiated SASD at about 17 GHz for B along [010] for two different crystals.

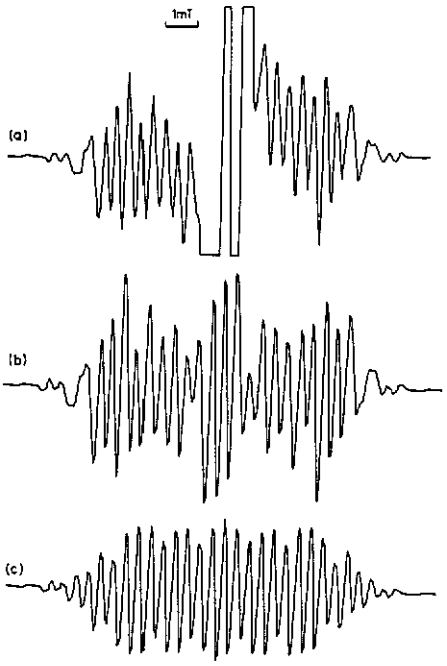

Figure 4. (*a*) Observed EPR spectrum at 300 K of x-irradiated SASD at about 9.4 GHz for B along [010] with a fraction of the protons isotopically substituted by deuterons. (*b*) simulated spectrum for parameters from table 2. (*c*) simulated spectrum without radical B (NH^+).

However, for reasons which we were not able to discover by any systematic search, there certainly were differences in spectra observed in different crystals at different times. A clear example of two different spectra for the [010] direction in different

crystals is shown in figure 3. This indicates that there are at least two types of spectra with extensive hyperfine structure, labelled A and B.

The strong lines at the centre of the spectrum correspond to two different species exhibiting no hyperfine structure. Type C is isotropic with $g = 2.0037$, and type D has the g-matrix given in table 1. These spectra, and those labelled A and B, have a linewidth of about 0.4 mT, typical of a dilute paramagnetic species in hydrated crystals, suggesting that it arises from unresolved hyperfine interaction with nearby protons. This is confirmed by much narrower lines in deuterated material (figure 4). There is a further spectrum (E) which is anisotropic both in position and linewidth. It is narrowest and most clearly observed for B in the [100] direction (figure 2), when the linewidth is 1.1 mT, independent of microwave frequency, and the same in a deuterated crystal. This is suggestive of unresolved hyperfine structure, possibly due to ^{23}Na. The g-matrix for E is given in table 1. There is also possibly a sixth, approximately isotropic, spectrum (F) with $g = 2.008$, which coincides with one of the inner hyperfine lines of spectrum B in figure 3 and makes it larger than other lines of spectrum B.

Table 1. Principal g-values and their directions for radicals D and E in x-irradiated SASD.

Radical	g-value	l	m	n
D	2.0018	−.5489	.1873	.8123
D	2.0063	.4356	−.7619	.4794
D	2.0098	.7134	.6170	.3322
E	2.0036	−.0832	.0515	.9952
E	2.0090	.2923	−.9535	.0738
E	2.0236	−.9527	−.2970	−.0643

The two spectra A and B are characterized by hyperfine separations of about 2.5 mT, the order of magnitude expected for α-protons in a radical such as NH_3^+. This assignment is confirmed by a reduction to a hyperfine separation of about 0.4 mT for a deuterated crystal. In addition to deuterated crystals, measurements were also made on crystals containing mainly ^{15}N, in an attempt to recognize the species giving the complicated hyperfine structure. This was confused by the fact that different crystal batches tended after irradiation to contain the different radical species in different proportion, so isotopic substitution did not produce the clear results one might have expected.

A careful comparison of the isotopically substituted crystals and the simpler spectra for all the crystallographic axes at several microwave frequencies between 9.4 and 35 GHz, in addition to as much information as could be obtained from the angular variation in the planes of reflection symmetry, led to an identification of the spectra. Radical A has hyperfine interaction with one N nucleus and three H nuclei: NH_3^+. Radical B had hyperfine interaction with one N and one H nucleus: NH^+. So far as we were able to follow the angular variation, it indicates an isotropic g-value of 2.0037 for both radicals and hyperfine matrices $\mathbf{A}_N$ for ^{14}N given in table 2. For NH^+, $\mathbf{A}_H$ appears to be isotropic ($A_H/g\mu_B = 2.2$ mT), while for NH_3^+ there is a small ($\simeq$ 8%) anisotropy in $A_H/g\mu_B$ with a mean value of $\simeq 2.5$ mT. These parameters are similar to those found by other workers for these radicals in other systems, except that for NH^+ there has usually been considerable anisotropy in A_H (Barbur 1971, Morton 1963, Rowlands 1962).

Table 2. Principal values of the hyperfine matrix $\mathbf{A}_N$ and their directions for ^{14}N in radicals $A(NH_3^+)$ and $B(NH^+)$ in x-irradiated SASD. The hyperfine matrix $\mathbf{A}_H$ for ^1H showed some small anisotropy about a value of approximately 2.4 mT.

Radical	$A/g\mu_B$ (mT)	l	m	n
A	0.27	−.908	−.066	.413
A	2.48	.380	−.542	.750
A	2.93	.175	.838	.517
B	0.71	−.868	−.069	.429
B	3.61	.250	−.917	.313
B	4.18	−.429	−.394	−.813

The interpretation of spectra from deuterated crystals is complicated by their contamination by a substantial fraction of protons. The radicals in them are therefore only partially deuterated, and the spectra are a superposition of a large number of lines (figure 4). Only towards the outer edges of the spectrum are the lines produced by only a few varieties of the radicals. Even there the overlap of spectra from different radicals makes the interpretation of the intensities of most of the lines difficult. In order to confirm the interpretation, the spectra were simulated on a computer treating the relative concentration x of the two species A and B as a variable. The relative concentrations of the partially deuterated species were taken to be those expected statistically for a proportion y of D replaced by H. The hyperfine parameters A_N and A_D were treated as variables. The g-values of the two radicals were assumed to be equal, and the line shape was assumed to be Gaussian with a linewidth taken from the experimental data.

For $\boldsymbol{B}$ along [010] it was not possible to match the observed spectrum without some contribution from radical $B(NH^+)$. The simulated spectra were a good fit to the experimental spectrum for the parameters given in table 3. However, for $\boldsymbol{B}$ parallel to [100] and [001] it was possible to simulate the spectra without any contribution from radical B; the parameters for NH_3^+ are also given in table 3, where it has been assumed that the values of y for the two batches are the same as used in the simulation for [010]. There is excellent agreement with the parameters for this radical from undeuterated material.

Table 3. Hyperfine line separations in mT for the two batches of deuterated crystals, 1 and 2, and for SASD (3).

Parameters for $\boldsymbol{B}$ along [010]

Batch	$A_N(NH_3)$	$A_D(NH_3)$	$A_H(NH_3)$	$A_N(NH)$	$A_D(NH)$	$A_H(NH)$	y	x
1	3.0	0.40	2.6	3.8	0.34	2.2	0.27	0.5
2	3.0	0.40	2.6	3.8	0.34	2.2	0.17	0.7
3	2.8		2.6	3.7		2.2		

Parameters for $\boldsymbol{B}$ along [100] and [001]

Direction		[100]			[001]	
Batch	A_N	A_D	A_H	A_N	A_D	A_H
1 & 2	1.2	0.37	2.4	2.5	0.37	2.4
3	1.1		2.2	2.5		2.4

The absence of radical B from the spectra in these two directions is puzzling. For

slight misorientation, the different angular dependencies of the spectra of the two radicals may enable the four symmetry-related spectra for NH_3^+ to be coincident while those for NH^+ are not, reducing the relative intensity of the latter. Another possibility is that $A_N(NH^+)$ is close to zero for these two directions, making the parameters for this radical almost identical to those found by Barbur (1971). However, although the latter explanation cannot be contradicted by the spectrum in figure 2(*a*) for [100], it is not possible to account for the lines in figure 2(*b*) for [001] with $A_N(NH^+) \simeq 0$.

One possible way of attempting to elucidate the hyperfine structure, and indeed to simplify the spectrum, would be to use ENDOR. For example, a sweep through the EPR spectrum while detecting the ENDOR of a particular nucleus in a particular radical, should display the EPR of that radical only. However, the signal/noise ratio of the hyperfine lines in our spectrum was far too small to make ENDOR feasible, particularly at temperatures above the ferroelectric transition.

4. Temperature dependence of the EPR spectrum

The only change observed in the spectrum on cooling through the transition temperature, was some evidence of doubling of the outermost hyperfine lines of HN_3^+. Any such doubling of the inner lines would be obscured by overlap with other spectra. Hence, it is impossible to say whether this arises from changes in the g-matrix, $\mathbf{A}_N$ or $\mathbf{A}_H$, or all three; or it could arise from a change in the motional averaging of the proton hyperfine structure making $\mathbf{A}_H$ anisotropic. In the absence of a clear interpretation of the hyperfine structure it was not profitable to pursue this further. In previously studied sulphates, structural changes at T_c were observed to cause a discontinuous change in the spectra of SO_4^- (or SeO_4^- in SASeD). Unfortunately the spectrum in SASD which we tentatively associate with SO_4^- is far too weak, and that for $Ns^{2+}SO_4$ far too wide, for any splitting to be observed. No obvious changes were observed in the stronger spectra without hyperfine structure. Hence, it does seem clear that any changes at T_c in the spectra of SO_2^-, SO_3^- and NH^+ are quite small, which may indicate that these radicals are sufficiently detached from the rest of the lattice that their structure is unaffected by any structural changes in the lattice.

5. Models for the sites produced by irradiation

It is interesting to compare our spectra with those found in SASeD (Ramani and Srinivasan 1981), in which no radicals were found with ^{14}N or ^1H hyperfine structure, but only SeO_4^-, SeO_3^- and SeO_2^-, the latter two being recognizable from ^{77}Se hyperfine structure. In our crystals any hyperfine structure from the 0.75% abundant ^{33}S would be swamped by the strong hyperfine lines in spectra A and B. The lack of hyperfine structure makes radicals C, D, E and F difficult to identify with certainty. The g-matrix is the only experimental information, which may be compared with the g-matrices found in other irradiated sulphates: comparison with the g-matrices for SeO_n^- is not helpful because the spin–orbit coupling in Se, being 4.4 times larger than that in S, causes much larger deviation from the free spin g-value; and significant contribution from d orbitals adds further complication. Table 4 lists various radicals which have been reported for irradiated sulphates.

SO_4^- has most frequently been reported with the hole shared between two oxygens, as in K_2SO_4, which leads to one relatively large principal g-value, whose value varies

Table 4. g-values of radicals found in various irradiated sulphates, together with those measured in SASD.

Radical	Host	Ref.	g_1	g_2	g_3	g_{av}
SO_4^-	K_2SO_4	[a]	2.0486	2.0082	2.0037	2.0202
	$K_2S_2O_8$	[b]		isotropic		2.0082
	NH_4HSO_4	[c]		isotropic		2.0078
SO_3^-	$K_2CH_2(SO_3)_2$	[d]		isotropic		2.0036
SO_2^-	Na_2SO_4	[e]	2.0102	2.0075	2.0013	2.0063
SO_2^+	$SrSO_4$	[f]	2.022	2.011	2.007	2.013
Na^+SO_2	$NaSO_4$	[g]	2.0101	2.0060	2.0024	2.0062
C	SASD			isotropic		2.0037
D	SASD		2.0098	2.0063	2.0018	2.0060
E	SASD		2.0236	2.0090	2.0036	2.0121
(F)	SASD		(2.008)			

[a] Morton *et al* (1966)
[b] Atkins *et al* (1963)
[c] Barbur (1971)
[d] Chantry *et al* (1962)
[e] Hariharam and Sobhanadi (1970)
[f] Samoilorich *et al* (1968)
[g] Adrian *et al* (1973)

from material to material: the g-matrix depends strongly upon the local environment, especially upon hydrogen bonding which governs the extent of delocalization between oxygen ligands. For NH_4HSO_4 the g-value is isotropic.

Of the radicals we observe, E is closest to the anisotropic SO_4^- spectrum, though g_1 is somewhat smaller than that for K_2SO_4. The principal directions of the g-matrix for this radical should be oriented with g_1 along the line joining two of the oxygen ligands, between which the hole is shared, and with g_3 oriented along the line joining the other two oxygen ligands. The directions for the g-matrix of E are close to the direction O(3)–O(4) for g_1 and O(2)–O(1) for g_3. However, the line is much wider than expected for SO_4^-. The line width of 1.1 mT, independent of microwave frequency, suggests unresolved ^{23}Na hyperfine structure: Na^+SO_2 was found for the g_1 direction to have a four-line hyperfine structure with overall spacing 0.74 mT. Although the g-matrix for E is smaller to that for Na^+SO_2, it is closer to SO_4^-. In our system, as one of the SO_4 oxygens O(4), is shared between two Na^+ ions, and as this is one of the oxygens which share the hole, it seems possible that radical E could be $Na_2SO_4^+$, giving a hyperfine interaction with both sodium nuclei.

Radical C, the strongest in our spectrum, with an isotropic g-value, seems likely to be SO_3^-. Radical D, the second strongest in our spectrum, has a g-matrix very close to that for SO_2^-. It seems likely that these radicals should occur in our spectra as SeO_3^- and SeO_2^- occur in SASeD.

One might expect that the spectrum produced by irradiation of $NaNH_4SO_4 \cdot 2H_2O$ should be similar to that of irradiated HNH_4SO_4 observed by Barbur (1971). There is close similarity between the spectra of Barbur's figure 1 and our figure 2(*b*). However, Barbur found the central isotropic line due to SO_4^- to lie at $g = 2.008$. Although we do not find a strong line at $g = 2.008$, the weak spectrum F may correspond to this.

The occurrence of only NH_3^+ and NH^+, derived from NH_4, in our irradiated crystals suggests a stability for singly charged positive ions: NH_4^+ and NH_2^+ are diamagnetic, and would give an EPR spectrum only if they captured an electron or a

hole.

It is interesting that γ-irradiation of SASeD does not produce radicals derived from NH_4. X- or γ-irradiation cannot directly produce atomic displacements, so the production of NH_x^+ and SO_x^- radicals must arise from radiolysis, after electron and hole production by the primary irradiation. That radicals of both types are produced in SASD and of only one type in SASeD, must imply either a preferential route of higher probability for SeO_4 than for SO_4, or that in-grown impurities or defects before irradiation are different in the two materials.

6. Conclusions

We have found, unlike in most other similar systems, very complicated EPR spectra in irradiated crystals of SASD. None of these spectra shows a marked change at T_c. This has been taken to indicate that all of the paramagnetic species observed are somewhat detached from the lattice in which they are embedded. The complexity of the EPR spectrum, combined with the very small changes in the spectrum, makes it impossible to extract information about structural changes at T_c with any certainty. Another noticeable feature of SASD is a marked sensitivity of the relative concentrations of the different paramagnetic species to unknown factors in the crystal growth.

References

Adrian F J, Cochran E L and Bowers V A 1973 *J. Chem. Phys.* **59** 56

Aleksandrov K S, Alexandrova I P, Shabanov V F, Yuzvak V I, Nozik Y Z and Fikin L I 1978 *Phys. Status Solidi* (a) **45** 53

Atkins P, Symons M C R and Trualino P A 1963 *Proc. Chem. Soc.* 222

Baker J M, Cook M I, Tronconi A L, Kuriata J and Sadlowski L 1992 abstract for 26th Congress AMPERE, Athens, p 488

Barbur I 1971 *Phys. Status Solidi* (b) **45** K129

Chantry G W, Horsefield A and Whiffen J R 1962 *Mol. Phys.* **5** 233

Corazzo E, Sabelli C and Guiseppetti G 1967 *Acta Crystallogr.* **22** 683

Genin D J and O'Reilly D E 1969 *J. Chem. Phys.* **50** 2842

Hariharam N and Sobhanadi J 1970 *J. Mol. Phys.* **18** 713

Lakshmana Rao J, Murali Krishna R, Lakshman S V J and Prem Chand 1990 *J. Phys. Chem. Solids* **51** 323

Makita Y and Sekido T 1965 *J. Phys. Soc. Japan* **20** 954

Morton J R 1963 *J. Phys. Chem. Solids* **24** 209

Morton J R, Bishop D M and Radnic M 1966 *J. Chem. Phys.* **45** 1885

Owens F J 1985 *Phase Transitions* **5** 81

Ramani K and Srinivasan R 1981 *Mol. Phys.* **44** 125

Rowlands J R 1962 *Mol. Phys.* **5** 565

Sadlowski L, Kuriata J and Lembicz F 1985 *Proc. RAMIS-85 (Adam Mickiewics University, Poznań, 1985)* ed N Pislewski p 411

Samoilorich M I, Norozhilov A I, Benov L V and Andrisenko N I 1968 *Radiokhimiya* **10** 506